Exposure to ultraviolet radiation causes apoptosis in developing sea urchin embryos

Michael P. Lesser*, Valerie A. Kruse and Thomas M. Barry

Department of Zoology and Center for Marine Biology, University of New Hampshire, Durham, NH 03824, USA

*Author for correspondence (e-mail: mpl@cisunix.unh.edu)

Summary

Laboratory exposures of embryos from the sea urchin *Strongylocentrotus droebachiensis* to ultraviolet B radiation (UV-B, 290–320 nm), equivalent to a depth of 1–3 m in the Gulf of Maine, resulted in significant damage to DNA measured as cyclobutane pyrimidine dimer formation. Cells with DNA damage caused by ultraviolet radiation (UVR, 290–400 nm) and oxidative stress can survive, but are often retained in the G_1/S phase of the cell cycle to repair DNA as a result of the expression of cell cycle genes such as *p*53 and *p*21, and the subsequent inhibition of the activity of cyclin-dependent kinases such as cdc2; if DNA cannot be repaired it can lead to programmed cell death or apoptosis. Sea urchin embryos exposed to UV-B radiation exhibit significantly higher protein concentrations of the antioxidant enzyme superoxide dismutase, and the transcriptional activators *p*53 and *p*21. The downstream activator of the cell cycle, cdc2, showed significantly lower protein concentrations with exposure to increasingly shorter wavelengths of UVR. Decreases in cdc2 could have been caused directly by exposure to UV-B or as a result of downregulation *via* the *p*53, *p*21 cascade, or both. These cellular events lead to apoptosis, as shown by the significant increase in DNA strand breaks observed in the nuclei of developing embryos exposed to UVR using the TUNEL assay. Cellular death, and a decrease in sea urchin embryo survivorship, are caused by the indirect and direct effects of exposure to UVR that leads to apoptosis in these laboratory experiments.

Key words: ultraviolet radiation, DNA damage, *p*53, apoptosis, oxidative stress, cell cycle, sea urchin, *Strongylocentrotus droebachiensis*.

Introduction

Despite decreases in the amount of ozone-depleting compounds, ozone depletion worldwide is expected to continue for the next half century with its co-occurring increase in the amount of harmful ultraviolet-B radiation (UV-B, 290–320 nm) reaching the biosphere (Madronich, 1998). UV-B radiation in temperate latitudes is estimated to have increased by 4–7% compared to values measured in the 1970s (Madronich, 1998). In the Gulf of Maine, the transmission of UV-B radiation varies significantly but can penetrate to depths of 7–12 m, depending on the optical properties of the water column (Banaszak et al., 1998; Lesser et al., 2001; Apprill and Lesser, 2003). The harmful effects of ultraviolet radiation (UVR) include damage to DNA, proteins and membrane lipids (Halliwell and Gutteridge, 1999), which affect a wide variety of marine organisms (Cullen et al., 1992; Gleason and Wellington, 1993; Herndl et al., 1993; Lesser et al., 1996; Shick et al., 1996; Franklin and Forster, 1997).

Surface waters of temperate near-shore coastal habitats (<10 m) contain the planktonic life-history phases of many species of fish, macrophytes and benthic invertebrates. Several species of echinoderms are important broadcast-spawning members of benthic communities in the Gulf of Maine and may therefore be susceptible to the detrimental effects of UVR. Exposure to UVR affects fertilization success, the timing of cleavage and development time for embryos and larvae of the green sea urchin *Strongylocentrotus droebachiensis* (Adams and Shick, 1996, 2001; Lesser and Barry, 2003). Many of the embryos and larvae survive these exposures, but in the study by Lesser and Barry (2003) all developmental stages tested exhibited significant DNA damage, measured as cyclobutane pyrimidine dimers (CPDs), which was highly correlated with delays in cell division and developmental delays. It was proposed that reactive oxygen species (ROS), formed by the univalent reduction of molecular O_2, and including singlet oxygen ($^1O_2$), superoxide radicals (O_2^-), hydrogen peroxide (H_2O_2) and hydroxyl radicals (HO·), formed *via* photodynamic action (Asada and Takahashi, 1987; Fridovich, 1986; Halliwell and Gutteridge, 1999; Valenzeno and Pooler, 1987), act synergistically with the direct effects of UVR to cause extensive DNA damage. This DNA damage leads to the expression of characteristic markers of the cell cycle such as *p*53 and *p*21 that result in delays in cell division while DNA

repair is taking place. DNA damage, followed by *p*53 expression, has also been observed in the embryos of the Atlantic cod (Lesser et al., 2001). If DNA repair is unsuccessful then those cells of the developing embryo are slated for apoptosis or programmed cell death pathways. Here, we provide evidence to support this hypothesis using embryos of the green sea urchin *S. droebachiensis*. We show that DNA damage is caused directly by exposure to UVR and provide evidence that DNA damage also occurred indirectly *via* the production of ROS. In addition to this DNA damage we observed differential expression of antioxidant and cell cycle genes and a positive response to the TUNEL assay, which are consistent with the onset of apoptosis in the cells of developing urchin embryos exposed to UVR.

Materials and methods

Experimental animals

Adult green sea urchins *Strongylocentrotus droebachiensis* Müller were collected from around the Isles of Shoals, Gulf of Maine (42°59.29′N, 70°37.01′W) at a depth of 10 m in March, 2001. All animals were brought back to the University of New Hampshire Coastal Marine Laboratory where they were maintained in seawater at 4–5°C. Animals were not fed and all were used within 2 weeks of collection. Reproductively mature animals were brought into the laboratory and induced to spawn by intracoelomic injection of 0.5 mol l^{-1} KCl at 4°C. Eggs from at least five females were combined and washed three times with 0.22 μm filtered seawater and collected using a 100 μm Nitex filter after each wash. Sperm were left 'dry' until used, and the sperm from at least three males was combined and diluted in 0.22 μm filtered seawater at ~1:10,000 to fertilize eggs at a density of 500 individuals ml^{-1} in 2 l sterile plastic containers (Corning, Inc., Corning, USA). After 5 min freshly fertilized embryos (FFE) were washed to remove excess sperm and maintained at a density of 20–30 individuals ml^{-1} until used for experiments. *Strongylocentrotus droebachiensis* FFE were used within 15 min of fertilization in experimental exposures to UVR and samples taken at this time showed a fertilization success of over 95% (three subsamples of 5 ml; 100 embryos counted per sample). In other experiments, *S. droebachiensis* embryos were allowed to develop to blastula and gastrula stages and then exposed to UVR as described below. Embryos were aerated and gently stirred using magnetic stir bars.

Embryo experiments

Freshly fertilized embryos, blastula, and gastrula stages were exposed to artificial visible radiation and UVR (290–700 nm wavelength) using four UV-340 lamps (Q-Panel, Cleveland, USA) and four F40 Sun lamps (General Electric) suspended ~15 cm from the top of the filters (see below) to provide a downwelling mixed field (visible and UVR) exposure. The effects of UVR were tested on embryos in 400 ml glass beakers at a density of 4–5 individuals ml^{-1}. Five treatments were used to partition the effects of UV-B from UV-A (320–400 nm) and visible radiation with three replicates per

treatment. WG and GG long-pass filters (Schott, Yonkers, USA) (6″×6″) with nominal cutoffs (50% transmission) at 280, 305, 320, 375 and 400 nm were used to cover the beakers containing embryos. Embryos were subjected to a 12.00 h:12.00 h light:dark cycle and experiments carried out for 3 days. Using this design, successive replicate experiments were carried out using embryos at different developmental stages for *Strongylocentrotus droebachiensis*. At the end of 3 days all embryos were collected for analyses as described below.

Measurements of ultraviolet radiation

For laboratory experiments UVR (UV-B and UV-A) and photosynthetically active radiation (PAR, 400–700 nm) were measured using a wavelength- and radiometrically calibrated [using National Institute of Standards and Technology (NIST) traceable standards] CCD spectrometer with fiber optics (Ocean Optics, Inc., Dunedin, USA). Three scans were taken and the mean values (W m^{-2} nm^{-1}) determined. Integrated values of unweighted UVR (W m^{-2}) were calculated for each treatment and biologically weighted irradiances (W m^{-2}) were obtained by multiplying the unweighted irradiance by the DNA weighting function of Setlow (1974).

Detection of DNA photoproducts using an enzyme-linked immunoabsorbent assay (ELISA)

Cyclobutane pyrimidine dimer (CPD) formation was measured using the procedures and monoclonal antibody (TDM-2) of Mori et al. (1991). Genomic DNA was isolated using commercially available kits (Easy-DNA, Invitrogen, Inc., Carlsbad, USA) and the quality and concentration determined spectrophotometrically using 260/280 nm ratios. Subsequently, 50 ng of DNA from each sample was used in an enzyme-linked immunoabsorbent assay (ELISA) technique with TDM-2 as the primary antibody and an affinity-purified goat anti-mouse IgG secondary antibody conjugated with horseradish peroxidase. The final color development was read in flat-bottomed 96-well microtiter plates using a plate reader (Bio-Rad, Inc., Hercules, USA) at 490 nm and the absorbance units reported as described by Mori et al. (1991).

Western blots

From the experiment described above, protein extracts of individual embryos (*N*=3) were homogenized using a tissue homogenizer in 10 mmol l^{-1} Hepes buffer, pH 7.5, containing dithiothreitol (DTT) and phenylmethylsulfonyl fluoride (PMSF) to prevent protein oxidation and certain classes of protease activity, respectively. The homogenate was then centrifuged at 500 *g* for 20 min and the supernatant saved for analysis of protein (Bradford, 1976). Samples (*N*=3) from each treatment of equivalent protein biomass were separated on SDS-PAGE gradient (4–15%) polyacrylamide gels and then transferred to PVDF membranes (0.2 μm). The membrane was blocked with 10% instant milk and immunoblotted using polyclonal antibodies against cytosolic superoxide dismutase (SOD), a polyclonal antibody to human *p*53 (23-mer; Kelly et

al., 2001), *p*21 (Santa Cruz Biologicals, Santa Cruz, USA) and cdc2 (*p*34, Santa Cruz Biologicals). The immunoblot was then developed using a secondary antibody, at a titer of 1:2000, labeled with horseradish peroxidase. Immunoblots of cdc2 were only performed on experiments with FFE because of the lack of sufficient biomass in the other developmental stages. The immunoblots were scanned and the optical density of the positive bands measured using a calibrated gray scale and the gel-scanning procedures described in NIH Image (version 1.61).

TUNEL assay

One of the diagnostic features of apoptosis is extensive damage to chromatin and DNA cleavage that leads to DNA fragmentation *via* an endogenous endonuclease. Identifying apoptotic cells can be accomplished using an *in situ* enzymatic end-labeling technique known as the TUNEL (TdT-mediated dUTP nick-end labeling) assay. Smears of experimental freshly fertilized embryos were made on clean glass slides and allowed to air dry. The cells were then fixed in buffered 4% paraformaldehyde for 1 h at 20°C. Cells were permeabilized using 0.1% Triton X-100, 0.1% sodium citrate in phosphate-buffered saline (PBS) at pH 7.4 and 4°C. Slides were rinsed in PBS (×3) and the 3′-OH termini of the DNA strand breaks labeled with modified nucleotides in an enzymatic reaction (In Situ Cell Death Detection Kit, Fluorescein, No. 1 684 795; Roche, Palo Alto, USA). The fluorescein-labeled DNA strand brakes in the nuclei of individual cells were then observed and scored using epifluorescence microscopy. Slides were covered with low fluorescence immersion oil and individual cells (*N*=200) from each treatment group with distinct nuclear end labeling (green emission at 515–565 nm) were scored as positive cells.

Statistical analysis

CPD formation and the optical density of the positive western blots were statistically analyzed using a one-way analysis of variance (ANOVA) at a significance level of 5%. No unequal variances were detected using the F_{max} test, and individual treatment differences were assessed using the Student–Newman–Keuls (SNK) multiple comparison test. Where appropriate, ratios and percentages were arcsine- or log-transformed for analysis and back-transformed for presentation. The TUNEL assay data were scored as positive and negative cells and analyzed using the non-parametric, multi-comparison Kruskal–Wallis test with Bonferroni/Dunn *post-hoc* comparisons, with an adjusted significant *P* value of 0.005 to control for experiment-wise Type I error.

Results

Table 1 shows the UVR irradiances for each treatment together with the total dose for the experiments on the embryos of *Strongylocentrotus droebachiensis*. The PAR irradiance was ~70 µmol quanta m^{-2} s^{-1} for all treatments. Additionally, the biologically effective irradiance (Table 1) for each treatment was calculated using the DNA damage weighting function of Setlow (1974). The maximum unweighted irradiance of UV-B is equivalent to that measured in coastal Gulf of Maine waters at a depth of 1–3 m.

Embryos of *Strongylocentrotus droebachiensis* exhibited significantly greater damage to DNA (ANOVA, *P*<0.001 on log-transformed values), measured as CPD formation (Fig. 1), at the end of the experimental UVR exposures. Multiple comparisons testing of the data from individual experiments at different embryonic stages showed that significantly more CPD formation occurred in the UV-B portion of the spectrum, while treatments without any UVR (GG 400 filter) always showed the lowest concentration of CPDs (SNK, *P*<0.05; Fig. 1).

Western blots revealed a single band at 17 kDa, which

Table 1. *Unweighted experimental irradiances and total dose for each treatment group and DNA weighted irradiances and dose using the DNA damage biological weighting function of Setlow (1974)*

Treatment wavelength (nm)	UVR		UV-A		UV-B	
	Irradiance (W m^{-2})	Dose (kJ m^{-2})	Irradiance (W m^{-2})	Dose (kJ m^{-2})	Irradiance (W m^{-2})	Dose (kJ m^{-2})
Unweighted						
280	6.31	817	5.79	750	0.52	67
305	5.93	768	5.68	736	0.35	45
320	5.79	750	5.45	706	0.25	32
375	0.85	110	0.84	108	0.001	0.13
400	0.0828	11	0.0826	11	0.0002	0.026
Weighted						
280	2.31×10^{-3}	0.299	1.46×10^{-5}	0.0019	2.30×10^{-3}	0.298
305	9.37×10^{-4}	0.121	1.33×10^{-5}	0.0017	9.24×10^{-4}	0.120
320	2.97×10^{-4}	0.038	1.29×10^{-5}	0.0017	2.83×10^{-4}	0.037
375	7.13×10^{-6}	0.0009	8.72×10^{-7}	0.00011	6.26×10^{-6}	0.0008
400	5.07×10^{-6}	0.0007	9.41×10^{-8}	0.00001	4.97×10^{-6}	0.0006

UVR, ultraviolet radiation (290–400 nm); UV-A, ultraviolet A radiation (320–400 nm); UV-B, ultraviolet B radiation (290–320 nm).
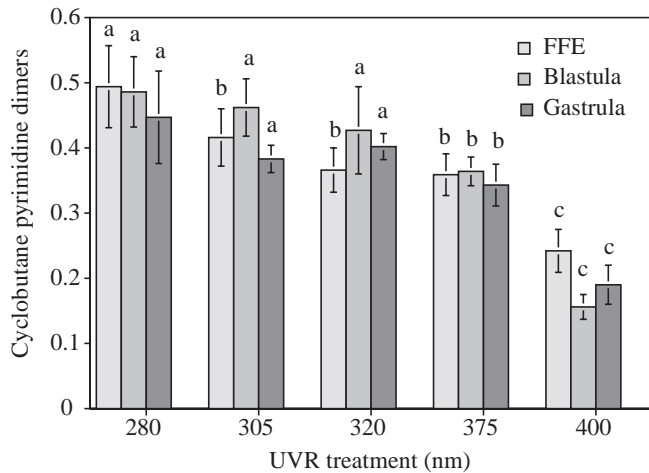Visible radiation (400–700 nm) was 70 µmol quanta m^{-2} s^{-1} for all treatments.

Fig. 1. DNA damage measured as cyclobutane pyrimidine dimers (means ± S.D.) of sea urchin (*Strongylocentrotus droebachiensis*) embryos exposed to UVR in the five treatment groups. Treatment groups that share superscripts within each developmental stage of the experiment are not significantly different from one another using multiple comparison testing (SNK) at a significance level of 0.05%.

corresponded to a Cu/Zn SOD standard (bovine erythrocytes; Sigma, Inc., St Louis, USA). Densitometer scans of SOD immunoblots showed that urchin embryos exposed to UVR expressed significantly greater concentrations of SOD (ANOVA, $P<0.05$) (Fig. 2A), with significant differences (multiple-comparison SNK, $P<0.05$) between the UV-B treatments (WG 280, WG 305 filters) and UV-A and control groups in most cases (Fig. 2A). Additionally, densitometer scans of immunoblots of the cell cycle genes *p53* and *p21* showed a similar significant (ANOVA, $P<0.05$) pattern of increasing *p53* (53 kDa) and *p21* (21 kDa) protein after exposure to UVR, especially the UV-B portion of the spectrum (SNK, $P<0.05$; Fig. 2B,C). The lone exception was the experiment on the gastrula stage, where *p21* showed a non-significant trend of increasing protein concentration with increasing UVR (ANOVA, $P=0.11$). Lastly, for the FFE of *Strongylocentrotus droebachiensis,* the densitometer scans of immunoblots for cdc2 (*p34*) showed an inverse and significant (ANOVA, $P<0.05$) pattern of decreasing protein concentration after exposure to UVR (Fig. 2D).

Experimental FFE showed a significantly (Kruskal–Wallis test; $P<0.001$ when corrected for ties) greater number of TUNEL-positive cells observed with DNA strand breaks (Fig. 3F). Embryos exposed to the shortest wavelengths of UV-B (280 nm, Fig. 3A) showed a greater percentage (36%) of TUNEL-positive cells than those in all other treatment groups (Bonferroni/Dunn test; $P<0.005$, 305 nm, 32%, Fig. 3B; 320 nm, 18%, Fig. 3C; 375 nm, 17%, Fig. 3D; 400 nm, 10%, Fig. 3E). Blastula- and gastrula-stage embryos showed a distinct difference between UV-B and UV-A wavelengths; UV-B exposed cells contained significantly more TUNEL-positive cells (blastula: 280 nm, 78%; 305 nm, 57%; 320 nm, 53%; gastrula: 280 nm, 100%; 305 nm, 61%; 320 nm, 54%)

than those exposed to longer wavelength UV-A (blastula: 375 nm, 37%; gastrula: 375 nm, 43%) or visible radiation only (blastula: 400 nm, 34%: gastrula: 400 nm, 29%) (Bonferroni/Dunn test; $P<0.005$) (not shown).

Discussion

Previous work on echinoid embryos revealed significant effects of UVR on cell division, development, morphology and DNA damage (Rustad, 1960; Eima et al., 1984; Akimoto and Shiroya, 1987). All of these studies, however, utilized artificial light sources containing germicidal UV-C (254 nm) radiation that is not ecologically relevant, as UVR below 290 nm does not reach sea level, but would result in significant damage to DNA, as indicated by the biological weighting function for DNA damage (Setlow, 1974). An action spectrum for cleavage delay after exposure to UVR showed a significant effect of wavelengths below 310 nm (Giese, 1939), again consistent with the biological weighting function for DNA damage (Setlow, 1974). More recent studies (Adams and Shick, 1996, 2001) have shown similar effects on urchin embryos after exposure to environmentally relevant wavelengths of UV-A and UV-B. Additionally, Lesser and Barry (2003) reported that environmentally relevant UVR had significant effects on echinoid survivorship, development, morphology and DNA damage. What has been generally lacking is an understanding of the underlying mechanism(s) causing cleavage delay, developmental abnormalities and cellular death after exposure to UVR.

DNA damage can be caused directly, by exposure to UVR as a result of absorbing photons of UVR, or indirectly, through the production of ROS (Imlay and Linn, 1988; Peak and Peak, 1990). This DNA damage can lead to the expression of *p53* (Renzing et al., 1996) and apoptosis or cellular necrosis in many organisms. Our results show an increase in the expression of SOD with exposure to UVR that is an indicator of an increase in superoxide radicals and other forms of ROS (Halliwell and Gutteridge, 1999; Pourzand and Tyrell, 1999). Oxidative stress is known to play a role in apoptosis *via* several cell cycle genes such as *p53* (Renzing et al., 1996). Two apoptotic pathways have been described and are known as the death-receptor pathway and the mitochondrial pathway. The mitochondrial pathway is commonly associated with DNA damage and upregulation or activation of the cell cycle gene *p53* (Hengartner, 2000). Exposure to UVR also causes ROS production in the electron transport chain of mitochondria (Gniadecki et al., 2000). Both the death receptor and mitochondrial pathways converge at the mitochondria and the Bcl-2 family of genes where the release of proapoptotic effectors (e.g. cytochrome *c*, ROS, caspase 9) occurs and subsequently leads to the assembly of the apoptosome, which among other things activates caspase-dependent DNase (Green and Reed, 1998; Rich et al., 2000).

The cell cycle checkpoint gene *p53* allows a multicellular organism to repair or delete cells exposed to agents that cause DNA damage, like hypoxia, UVR, ROS or mutagens (Graeber
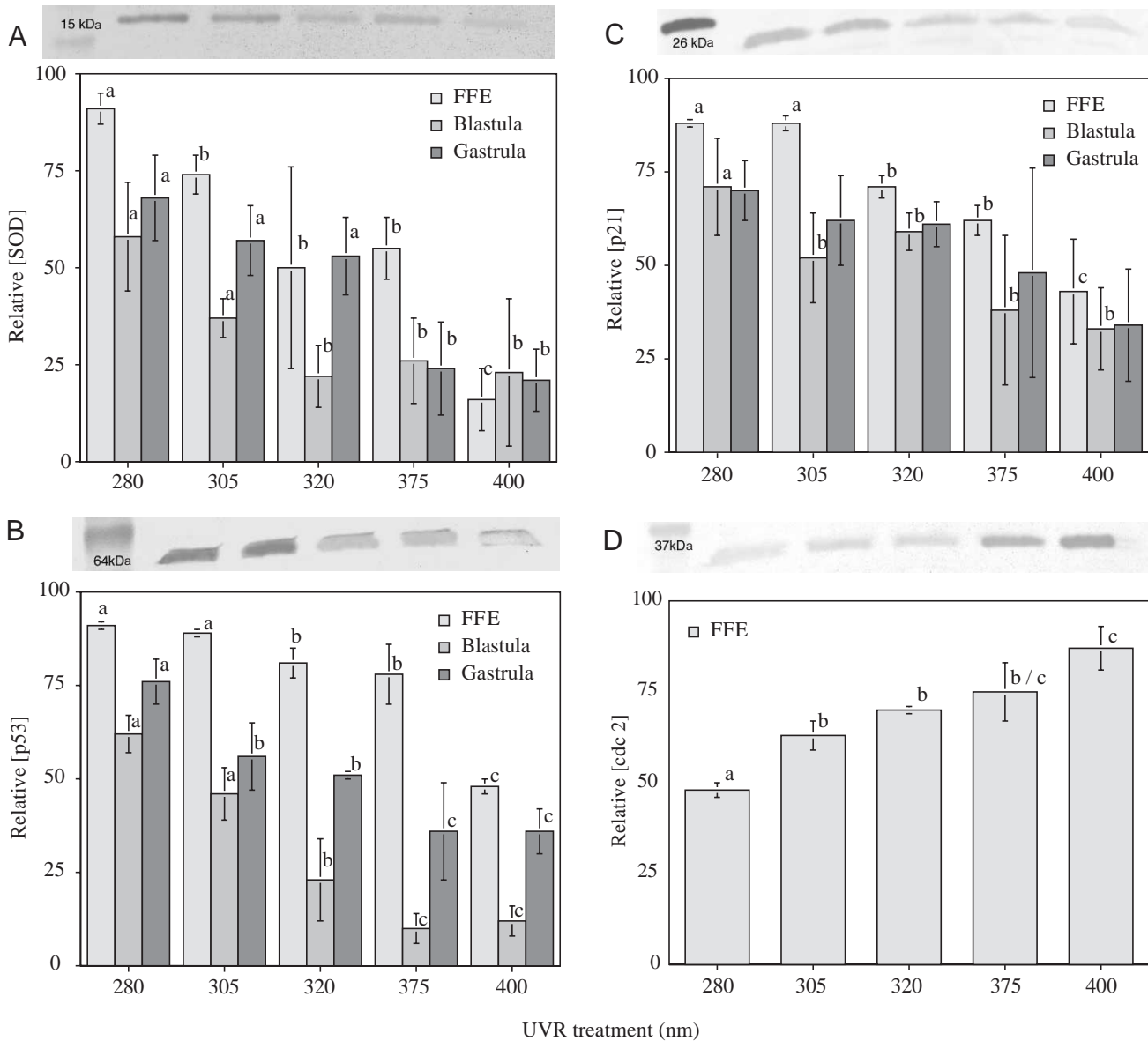
Fig. 2. (A) Superoxide dismutase protein (SOD) concentration measured as optical density (relative units) of immunoblots of sea urchin (*Strongylocentrotus droebachiensis*) embryos exposed to UVR in the five treatment groups. (B) *p*53 protein concentration measured as optical density of immunoblots of sea urchin (*Strongylocentrotus droebachiensis*) embryos exposed to UVR at five different wavelengths (treatment groups). (C) *p*21 protein concentration measured as optical density of immunoblots of sea urchin (*Strongylocentrotus droebachiensis*) embryos exposed to UVR in the five treatment groups. (D) cdc2 protein concentration measured as optical density of immunoblots of sea urchin (*Strongylocentrotus droebachiensis*) freshly fertilized embryos exposed to UVR in the five treatment groups. See representative immunoblot above each bar graph. *N*=3 samples for each treatment (i.e. filter); values are means ± S.D. of relative optical density. Treatment groups that share superscripts are not significantly different from one another using multiple comparison testing (SNK) at a significance level of 0.05%. FFE, freshly fertilized embryos.

et al., 1996; Renzing et al., 1996; Clarke et al., 1997; Griffiths et al., 1997). Upregulation and expression of *p*53 allows DNA editing and repair to occur followed either by normal cell division (Polyak et al., 1997) or apoptosis (Hale et al., 1996). Cells with DNA damage caused by UVR and oxidative stress can survive but are often retained in the G_1/S phase of the cell cycle for long periods of time (Geyer et al., 2000). These delays in cell division are the result of the expression of *p*53 and ultimately the downregulation of cyclin-dependent kinases

(Evan and Littlewood, 1998). An important pathway by which *p*53 facilitates an arrest in the cell cycle is through the *p*21 protein. *p*21 is an inhibitor of a wide range of kinases such as cdc2. *p*53 is also known to be regulatory at the G_2/M checkpoint through its effect on cyclin B1 after DNA damage (Innocente et al., 1999) and both *p*53 and *p*21 are required to sustain a G_2/M arrest after DNA damage (Bunz et al., 1998).

One diagnostic feature of apoptosis is extensive damage to chromatin and DNA cleavage, leading to DNA fragments *via*
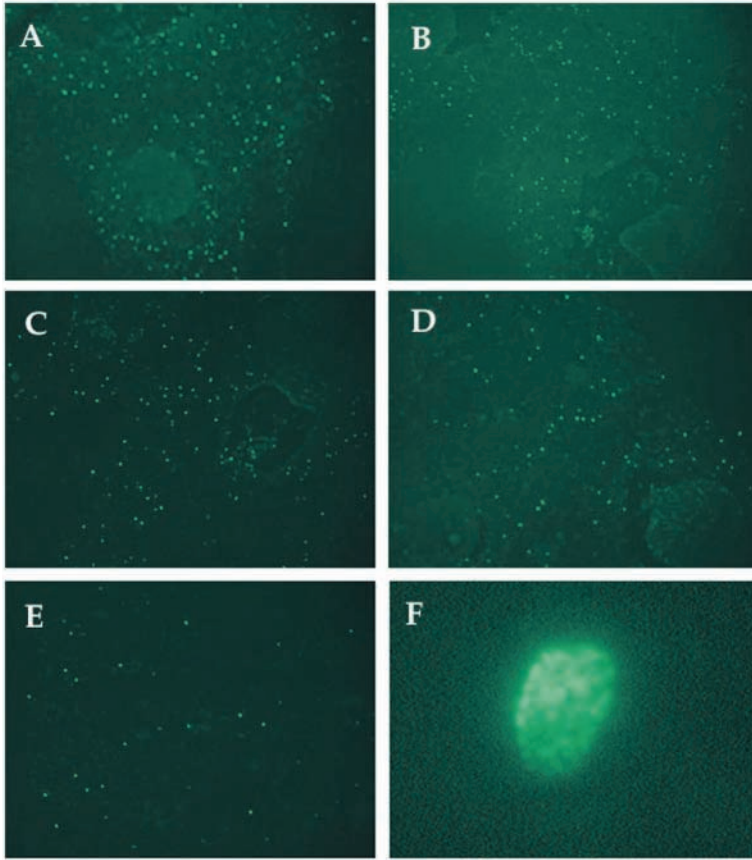
Fig. 3. Freshly fertilized embryos of the sea urchin *Strongylocentrotus droebachiensis* after exposure to UVR at five different wavelengths (treatment groups). DNA damage was assessed by TUNEL-positive fluorescence, which reveals cells with DNA strand damage. See text for details. (A) 280 nm, (B) 305 nm, (C) 320 nm, (D) 375 nm, (E) 400 nm. Magnification 100×. (F) Single nuclei after 280 nm treatment; magnification 5500×.

previously been shown in sea urchin embryos and larvae (Voronina and Wessel, 2001; Roccheri et al., 2002) and the results reported here for green sea urchin embryos reveal a significant increase in the number of apoptotic cells after exposure to UVR. While the work of Voronina and Wessel (2001) suggests that the TUNEL assay may underestimate the number of apoptotic cells, we feel that this underestimation would be systematic throughout our experiments and thus not affect the interpretation of UVR-induced apoptosis in the treatments described above. The TUNEL assay results are also strongly supported by the differential expression patterns of cell cycle and antioxidant proteins. Additionally, in these experiments and other studies (Adams and Shick, 2001; Lesser and Barry, 2003) the abnormal morphologies observed (e.g. 'packed' blastula, blebbing, exogastrulation) are consistent with descriptions of apoptotic morphology.

In summary, exposure of developing embryos of the green sea urchin to UVR causes a cascade of cellular events from DNA damage to apoptosis. Between these two events, well-described checkpoints and controllers of the cell cycle are regulated in a pattern that has been described for many metazoan systems. Additionally, the differential effects of UV-B *versus* UV-A are quite clear. Exposure to the shorter UV-B wavelengths, those affected by stratospheric ozone depletion, result in more DNA damage, higher levels of oxidative stress and greater expression of cell cycle genes that lead to apoptosis. We also see, however, significant effects on these processes from exposure to the UV-A portion of the spectrum, which has more total energy available and penetrates to deeper depths even in coastal temperate waters. Our results do not rule out the possibility of direct effects of UVR on critical proteins (e.g. cdc2), but the results presented here show that delays in cell division, abnormal development and, ultimately, the death of developing embryos begins with direct and indirect damage to DNA.

an endogenous endonuclease. The embryos of green sea urchins exposed to UVR exhibit both direct effects of UVR on DNA, as observed through the accumulation of CPD photoproducts, and the positive TUNEL assay, which indicates the occurrence of DNA strand breaks caused by ROS (Imlay and Linn, 1988; Pourzand and Tyrell, 1999). Subsequent to this DNA damage we observed a tight coupling between *p*53 and *p*21 expression that is functionally related to the delays in cell division observed in this species under similar conditions (Adams and Shick, 1996, 2001; Lesser and Barry, 2003). Additionally, the ultimate cell cycle regulator cdc2 shows a decrease in concentration with increasing exposure to UVR in freshly fertilized embryos. We believe this is either a consequence of the expression of *p*53 and *p*21, or a direct consequence of exposure to UVR, or both. In fact, inactivation of cdc2 has been shown to facilitate apoptosis induced by DNA damage (Ongkeko et al., 1995). When the results of the TUNEL assay are examined it is apparent that some cells, a significantly lower percentage, are apoptotic without having been exposed to UVR. A functional apoptotic pathway has

References

Adams, N. and Shick, J. M. (1996). Mycosporine-like amino acids provide protection against ultraviolet radiation in eggs of the green sea urchin *Strongylocentrotus droebachiensis*. *Photochem. Photobiol.* **64**, 149-158.

Adams, N. and Shick, J. M. (2001). Mycosporine-like amino acids prevent UV-B induced abnormalities during early development of the green sea urchin *Strongylocentrotus droebachiensis*. *Mar. Biol.* **138**, 267-280.

Akimoto, A. and Shiroya, T. (1987). Photoreversability of UV-induced thymine dimmers and abnormal morphogenesis in sea-urchin embryos. *Photochem. Photobiol.* **45**, 403-406.

Apprill, A. M. and Lesser, M. P. (2003). Effects of ultraviolet radiation on

Laminaria saccharina in relation to depth and tidal height in the Gulf of Maine. *Mar. Ecol. Prog. Ser.* **256**, 75-85.

Asada, K. and Takahashi, M. (1987). Production and scavenging of active oxygen in photosynthesis. In *Photoinhibition* (ed. D. J. Kyle, C. B. Osmond and C. J. Arntzen)*,* pp. 228-287. Amsterdam: Elsevier.

Banaszak, A. T., Lesser, M. P., Kuffner, I. B. and Ondrusek, M. (1998). Relationship between ultraviolet (UV) radiation and mycosporine-like amino acids (MAAS) in marine organisms. *Bull. Mar. Sci.* **63**, 617-628.

Bradford, M. M. (1976). A rapid and sensitive method for the quantitation of microgram quantities of protein using the principle of protein-dye binding. *Anal. Biochem.* **72**, 248-254.

Bunz, F., Dutriaux, A., Langauer, C., Waldman, T., Zhou, S., Brown, J. P., Sedivy, J. M., Kinzler, K. W. and Vogelstein, Z. B. (1998). Requirement for p53 and p21 to sustain G_2 arrest after DNA damage. *Science* **282**, 1497-1501.

Clarke, A. R., Howard, L. A., Harrison, D. J. and Winton, D. J. (1997). *p*53 mutation frequency in the murine small intestine. *Oncogene* **14**, 2015-2018.

Cullen, J. J., Neale, P. J. and Lesser, M. P. (1992). Biological weighting function for the inhibition of phytoplankton photosynthesis by ultraviolet radiation. *Science* **258**, 646-651.

Eima, Y., Ikenaga, M. and Shiroya, T. (1984). Action spectrum for photoreactivation of ultraviolet-induced morphological abnormality in sea urchin eggs. *Photochem. Photobiol.* **40**, 461-464.

Evan, G. and Littlewood, T. (1998). A matter of life and cell death. *Science* **281**, 1317-1322.

Franklin, L. A. and Forster, R. M. (1997). The changing irradiance environment: consequences for marine macrophyte physiology, productivity and ecology. *Eur. J. Phycol.* **32**, 207-232.

Fridovich, I. (1986). Biological effects of the superoxide radical. *Arch. Biochem. Biophys.* **247**, 1-11.

Geyer, R. K., Nagasawa, H., Little, J. B. and Maki, C. G. (2000). Role and regulation of p53 during ultraviolet radiation-induced G_1 cell cycle arrest. *Cell Growth Differ.* **11**, 149-156.

Giese, A. C. (1939). The effects of ultra-violet radiations of various wavelengths upon cleavage of sea urchins. *Biol. Bull.* **75**, 238-247.

Gleason, D. F. and Wellington, G. M. (1993). Ultraviolet radiation and coral bleaching. *Nature* **365**, 836-838.

Gniadecki, R., Thorn, T., Vicanova, J., Petersen, A. and Wulf, H. C. (2000). Role of mitochondria in ultraviolet-induced oxidative stress. *J. Cell. Biochem.* **80**, 216-222.

Graeber, A. G., Osmanian, C., Jack, T., Housman, D. E., Koch, C. J., Lowe, S. W. and Graccia, A. J. (1996). Hypoxia-mediated selection of cells with diminished apoptotic potential in solid tumors. *Nature* **379**, 88-91.

Green, D. R. and Reed, J. C. (1998). Mitochondria and apoptosis. *Science* **281**, 1309-1312.

Griffiths, S. D., Clarke, A. R., Healy, L. E., Ross, G., Ford, A. M., Wyllie, A. H. and Greaves, M. (1997). Absence of *p*53 permits propagation of mutant cells following genotoxic damage. *Oncogene* **14**, 523-531.

Hale, A. J., Smith, C. A., Sutherland, L. C., Stoneman, V. E., Longthorne, V. L., Culhane, A. C. and Williams, G. T. (1996). Apoptosis: molecular regulation of cell death. *Eur. J. Biochem.* **236**, 1-26.

Halliwell, B. and Gutteridge, J. M. C. (1999). *Free Radicals in Biology and Medicine,* 3rd edition. 936pp. Oxford: Oxford Science Publications.

Hengartner, M. O. (2000). The biochemistry of apoptosis. *Nature* **407**, 770-776.

Herndl, G. J., Müller-Niklas, G. and Frick, J. (1993). Major role of ultraviolet-B in controlling bacterioplankton growth in the surface layer of the ocean. *Nature* **361**, 717-719.

Imlay, J. A. and Linn, S. (1988). DNA damage and oxygen radical toxicity. *Science* **240**, 1302-1309.

Innocente, S. A., Abrahamson, J. L. A., Cogswell, J. P. and Lee, J. M. (1999). p53 regulates a G_2 checkpoint through cyclin B1. *Proc. Natl. Acad. Sci. USA* **96**, 2147-2152.

Kelly, M. L., Winge, P., Heaney, J. D., Stephens, R. E., Farrell, J. H., Van Beneden, R. J., Reinisch, C. L., Lesser, M. P. and Walker, C. W. (2001) Expression of homologues for p53 and p73 in the softshell clam (*Mya arenaria*), a naturally-occurring model for human cancer. *Oncogene* **20**, 748-758.

Lesser, M. P. and Barry, T. M. (2003). Survivorship, development, and DNA damage in echinoderm embryos and larvae exposed to ultraviolet radiation (290–400 nm). *J. Exp. Mar. Biol. Ecol.* **292**, 75-91.

Lesser, M. P., Neale, P. J. and Cullen, J. J. (1996). Acclimation of Antarctic phytoplankton to ultraviolet radiation: UV absorbing compounds and carbon fixation. *Mol. Mar. Biol. Biotech.* **5**, 314-325.

Lesser, M. P., Farrell, J. H. and Walker, C. W. (2001). Oxidative stress and p53 expression in the larvae of Atlantic cod (*Gadus morhua*) exposed to ultraviolet (290–400 nm) radiation. *J. Exp. Biol.* **204**, 157-164.

Madronich, S., McKenzie, R. L., Björn, L. O. and Caldwell, M. M. (1998). Changes in biologically active radiation reaching the Earth's surface. *Photochem. Photobiol.* **46**, 5-19.

Mori, T., Nakane, M., Hattori, T., Matsunaga, T., Ihara, M. and Nikaido, O. (1991). Simultaneous establishment of monoclonal antibodies specific for either cyclobutane pyrimidine dimers or (6-4) photoproduct from the same mouse immunized with ultraviolet radiated DNA. *Photochem. Photobiol.* **54**, 225-232.

Peak, M. J. and Peak, J. G. (1990). Hydroxyl radical quenching agents protect against DNA breakage caused by both 365-nm and gamma radiation. *Photochem. Photobiol.* **51**, 649-652.

Polyak, K., Xla, Y., Zweler, J. L., Kinzler, K. W. and Vogelstein, B. (1997). A model for *p*53 induced apoptosis. *Nature* **389**, 300-305.

Pourzand, C. and Tyrell, R. M. (1999). Apoptosis, the role of oxidative stress and the example of solar UV radiation. *Photochem. Photobiol.* **70**, 380-390.

Ongkeko, W., Ferguson, D. J. P., Haris, A. L. and Norbury, C. (1995). Inactivation of Cdc2 increases the level of apoptosis induced by DNA damage. *J. Cell. Sci.* **108**, 2897-2904.

Rich, T., Allen, R. L. and Wyllie, A. H. (2000). Defying death after DNA damage. *Nature* **407**, 777-783.

Renzing, J., Hansen, S. and Lane, D. P. (1996). Oxidative stress is involved in the UV activation of *p*53. *J. Cell Sci.* **109**, 1105-1112.

Roccheri, M. C., Tipa, C., Bonaventura, R. and Matranga, V. (2002). Physiological and induced apoptosis in sea urchin larvae undergoing metamorphosis. *Int. J. Dev. Biol.* **46**, 801-806.

Rustad, R. C. (1960). Changes in the sensitivity to ultraviolet-induced mitotic delay during the cell division cycle of the sea urchin egg. *Exp. Cell. Res.* **21**, 596-602.

Setlow, R. B. (1974). The wavelengths in sunlight effective in producing skin cancer: a theoretical analysis. *Proc. Natl. Acad. Sci. USA* **71**, 3363-3366.

Shick, J. M., Lesser, M. P. and Jokiel, P. L. (1996). Effects of ultraviolet radiation on corals and other coral reef organisms. *Global Change Biol.* **2**, 527-545.

Valenzeno, D. P. and Pooler, J. P. (1987). Photodynamic action. *BioScience* **37**, 270-276.

Voronina, E. and Wessel, G. M. (2001). Apoptosis in sea urchin oocytes, eggs, and early embryos. *Mol. Reprod. Dev.* **60**, 553-561.